Efficient rainbow color luminescence from InxGa1-xN single quantum wells fabricated on {11(2)over-bar2} microfacets

AUTHOR(S):

Nishizuka, K; Funato, M; Kawakami, Y; Narukawa, Y; Mukai, T

CITATION:

Nishizuka, K ...[et al]. Efficient rainbow color luminescence from InxGa1-xN single quantum wells fabricated on {11(2)over-bar2} microfacets. APPLIED PHYSICS LETTERS 2005, 87(23): 231901.

ISSUE DATE:

2005-12-05

URL:

http://hdl.handle.net/2433/50169

APPLIED PHYSICS LETTERS **87**, 231901 (2005)

Efficient rainbow color luminescence from $In_xGa_{1-x}N$ single quantum wells fabricated on {11$\bar{2}$2} microfacets

K. Nishizuka,[a] M. Funato, and Y. Kawakami
Department of Electronic Science and Engineering, Kyoto University, Kyoto 615-8510, Japan

Y. Narukawa and T. Mukai
Nitride Semiconductor Research Laboratory, Nichia Corporation, Tokushima 774-8601, Japan

(Received 3 August 2005; accepted 14 October 2005; published online 28 November 2005)

Rainbow color luminescence from $In_xGa_{1-x}N$ single quantum wells (SQWs) is achieved and almost covers the entire visible range when the layers are fabricated on {11$\bar{2}$2} facets with a few micron-width using a regrowth technique on striped GaN templates. These facets are tilted 56° with respect to the (0001) facets and border the (0001) and {11$\bar{2}$0} facets. The emission wavelength on the {11$\bar{2}$2} facets is redshifted from the {11$\bar{2}$0} side to (0001) side due to the variations of the In composition, which leads to the color contrast with the rainbow geometry. The temperature dependence of the photoluminescence intensity shows that the internal quantum efficiency at room temperature is 33% due to the very small internal electric fields and a small threading dislocation density compared to that in conventional (0001) $In_xGa_{1-x}N$ SQWs. Since the emission efficiency does not show a noticeable emission wavelength dependence, this type of structure has potential as light-emitting devices with multiwavelengths that perform numerous color controllability such as pastel and white colors. © *2005 American Institute of Physics*. [DOI: 10.1063/1.2136226]

Modern growth technology has paved the way towards blue light-emitting diodes (LEDs) based on $In_xGa_{1-x}N/GaN$ quantum wells (QWs). Since the band-gap energy of $In_xGa_{1-x}N$ can be tuned from 0.7 eV (InN)[1,2] to 3.5 eV (GaN), it can cover not only from near ultraviolet (UV) to full-visible light, but also to the infrared range by changing the In composition. However, the external quantum efficiency (η_{ext}) begins to decrease in the blue-green range as the emission wavelength increases despite the very high attainable η_{ext} value (~40%) for near-UV, violet, and blue LEDs. Actually, $In_xGa_{1-x}N$-based red LEDs show η_{ext} of only a few percent, which is insufficient for synthesizing white light from this material. This is, at least partially, due to the quantum confinement Stark effect[3,4] (QCSE) caused by strong piezoelectric polarization in strained $In_xGa_{1-x}N/GaN$ QWs oriented in the [0001] direction. Numerous groups have tried to fabricate $In_xGa_{1-x}N/GaN$ and $Al_xGa_{1-x}N/GaN$ QWs on nonpolar planes to avoid QCSE,[5–7] but the layers contain numerous nonradiative recombination centers (NRCs) since it is difficult to achieve a high crystallinity on nonpolar planes. Another approach is to use planes tilted with respect to the [0001] direction since theoretical calculations show that the magnitude of the piezoelectric field is reduced when the tilting angle (θ) is increased, becomes zero at $\theta=\theta_C$, changes polarity for $\theta>\theta_C$, and becomes zero again at $\theta=90°$. It is noteworthy that the estimated angle of θ_C deviates from 39° (Ref. 8) to 55°,[9] due to the scattering of the reported material parameters such as the piezoelectric constants and elastic constants. We recently proposed that the {11$\bar{2}$2} plane ($\theta=56°$) is promising for low internal electric fields when these planes naturally appear through the regrowth process on GaN templates patterned with a striped geometry.[10] It was determined that the radiative recombination lifetime of violet (400 nm) emission from the {11$\bar{2}$2}$In_xGa_{1-x}N/GaN$ QWs is ~380 ps at 14 K, which is 3.8 times shorter than that of conventional (0001) QWs. This suggests a well suppression of the internal electric fields. In this paper, multi wavelength (rainbow color) luminescence from the ⟨11$\bar{2}$2⟩-oriented $In_xGa_{1-x}N/GaN$ single QW (SQW) is demonstrated by controlling the variations of the In composition within this microfacet in order to show the effectiveness of these types of structures as tunable color LEDs.

The sample was grown on a sapphire (0001) substrate by metal-organic vapor phase epitaxy. Using a regrowth technique, GaN microstructures, which were composed of (0001), {11$\bar{2}$2}, and {11$\bar{2}$0} facets and elongated along the [1$\bar{1}$00] direction, were formed. Then $In_xGa_{1-x}N/GaN$ SQWs were fabricated on these microfacets. The detailed growth procedures have already been published in Ref. 10.

Figure 1(a) shows a cross-sectional scanning transmission electron microscopy (STEM) bright field image of a fabricated structure viewed along the [1$\bar{1}$00] direction. The specimen was prepared by conventional Ar^+ milling, and the acceleration voltage for the STEM observation was 200 kV.

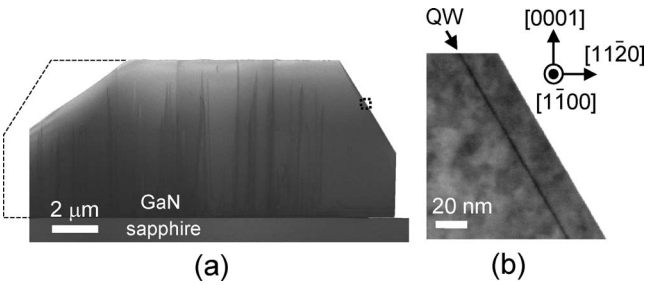

FIG. 1. [1$\bar{1}$00] Cross-sectional STEM bright field images viewed. (a) Entire region and (b) magnified image of the area designated by the dotted rectangle on the (11$\bar{2}$2) plane. The broken line in (a) indicates the original shape.

[a]Electronic mail: k-nishi@fujita.kuee.kyoto-u.ac.jp

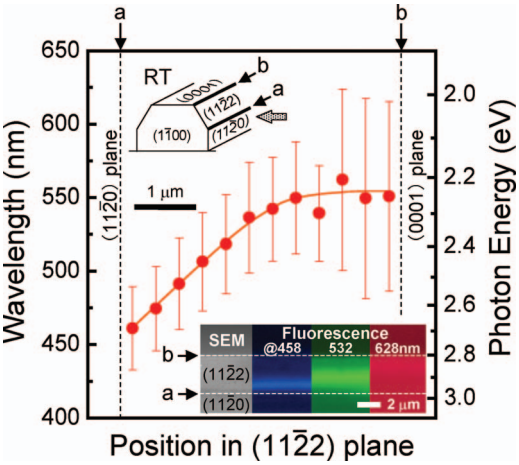

FIG. 2. (Color) Position dependence of the CL peak wavelength of the (11$\bar{2}$2) SQW. The error bars represent the emission line widths. The lower inset is a SEM image and monochromatic FLM images monitored at 458, 532, and 628 nm, while the upper inset shows a schematic sample structure where the arrow indicates the measurement direction.

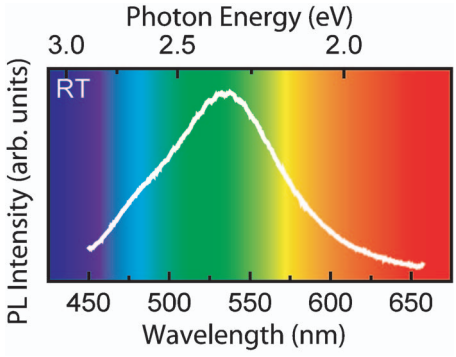

FIG. 3. (Color) PL spectrum of the {11$\bar{2}$2} SQWs measured at RT. The background color is equivalent to the emission colors.

The broken line on the left-hand side indicates the original shape, which was overmilled during specimen preparation. It was confirmed that the (0001), {11$\bar{2}$2}, and {11$\bar{2}$0} facets appeared. Almost all of the threading dislocations propagated toward the [0001] direction and some were bent by 90° toward the ⟨11$\bar{2}$0⟩ direction near the GaN/sapphire interface. Consequently, dislocations were barely observed on the {11$\bar{2}$2} facets, which can be advantageous for high emission efficiency since dislocations work as NRCs. A magnified image of the (11$\bar{2}$2) QW is shown in Fig. 1(b), the position of which is designated by the dotted rectangle in Fig. 1(a). The clear contrast indicated that an $In_xGa_{1-x}N$ well with a thickness of 2±0.2 nm was successfully formed and was uniform within the (11$\bar{2}$2) facet. On the other hand, the In composition was estimated by energy dispersive X-ray spectroscopy (EDS) equipped to the STEM system using the same procedure as in our previous study.[10] The composition monotonously increased from 25% on the (11$\bar{2}$0) side to 40% on the (0001) side. Considering a 2-nm uniform well width and an internal electric field due to the piezoelectric and spontaneous polarization, the estimated QW transition energy ranged from 2.43 eV (510 nm) to 2.79 eV (444 nm).

This surprisingly large distribution of the In composition was caused by the growth characteristics of $In_xGa_{1-x}N$ on GaN microfacets. The STEM observation revealed that the growth rate became faster in the order (0001)>{11$\bar{2}$2}>{11$\bar{2}$0}, suggesting that the atoms migrated from {11$\bar{2}$0} toward (0001) through the {11$\bar{2}$2} facet. Furthermore, since an In atom possesses a higher diffusivity than Ga atom due to a higher vapor pressure, the In composition gradually increased along the stream of In migration; that is, (0001)>{11$\bar{2}$2}>{11$\bar{2}$0}. More detailed growth characteristics will be discussed elsewhere.

The influence of this In spatial distribution in the {11$\bar{2}$2} QW on the optical properties was microscopically investigated by cathode luminescence (CL) and fluorescence microscopy (FLM) measurements at room temperature (RT). The inset of Fig. 2 shows the representative monochromatic FLM images together with scanning electron microscopy (SEM) image observed along the [11$\bar{2}$0] direction. For the monochromatic FLM images, bandpass filters with a bandwidth of 3 nm were used at the monitored center wavelengths of 458 (blue), 532 (green), and 628 nm (red). As shown, the emission band formed along the [1$\bar{1}$00] direction and moved toward the top (0001) facet while broadening its width with a longer monitored wavelength. Interestingly, blue, green, and red were observed from a single facet, suggesting that the luminescence from the {11$\bar{2}$2} QW covers the full-visible range. A more detailed position dependence was examined by CL, and Fig. 2 plots the CL peak wavelengths. The error bars represent the full width at half maximum (FWHM). The peak wavelength ranged from 460 nm (2.70 eV) to 551 nm (2.25 eV) from the (11$\bar{2}$0) side to the (0001) side, which is consistent with the above calculations based on STEM and EDS observations and suggests that the position dependence is due to the In spatial distribution. Furthermore, FWHM was ~60 nm (more than 200 meV), except for near the (0001) facet and suddenly broadened near the (0001) facet. This rather broad FWHM also supports the presence of a significant In distribution.

Macroscopic optical properties of the {11$\bar{2}$2} QWs were assessed by selectively exciting the wells with a frequency-doubled Ti:sapphire laser emitting 400 nm. The repetition rate, pulse width, and excitation density were 80 MHz, 1.5 ps, and 1.31 $\mu J/cm^2$, respectively. Figure 3 shows a PL spectrum acquired at RT. The PL peaked at 535 nm (2.32 eV), and covered wavelengths from 450 nm to 650 nm, which corresponds to almost the entire visible range. The estimated FWHM was ~450 meV, which is more than twice as large as a typical value for conventional *C*-oriented $In_xGa_{1-x}N$ QWs. This anomalously broad emission was due to the In spatial distribution and characterized the luminescence color of the present {11$\bar{2}$2} QWs. In terms of the CIE (Commission Internationale de l'Éclairage) chromaticity chart, it is classified into whitish emerald green, far from monochromatic light. Since the In distribution in a plane is controlled by the growth conditions, various apparent colors including white can be realized using only the structure proposed in this study. This is strikingly different from conventional technologies where the light color is designed by, for example, using several emitters with different output colors or using phosphors as a color converter.

It is noteworthy that some theoretical studies have indicated that $In_xGa_{1-x}N$ QWs with a crystalline tilt should have weaker internal electric fields and consequently, higher emis-

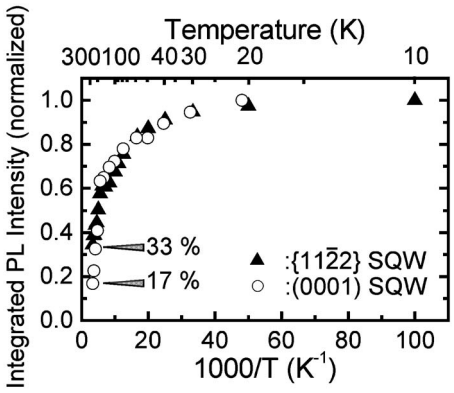

FIG. 4. Temperature dependence of the integrated PL intensity. The results for the {11$\bar{2}$2} SQWs (▲) and conventional (0001) SQW (○) are shown. The intensities are normalized by that at 13 K.

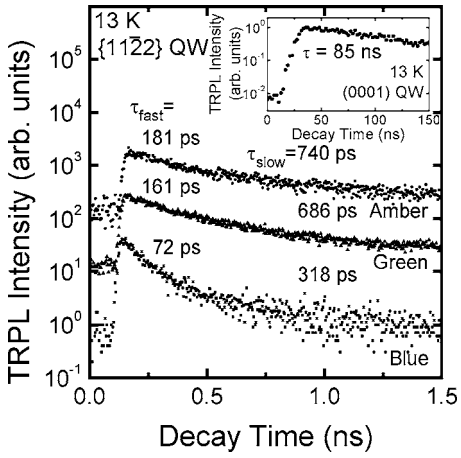

FIG. 5. PL decay curves of {11$\bar{2}$2} SQWs at 13 K monitored at 460 nm (blue), 530 nm (green), and 575 nm (amber). For comparison, the inset shows that for conventional (0001) SQW.

sion efficiency.[8,11] Our QW was directed toward ⟨11$\bar{2}$2⟩ tilted 56° from the [0001] direction. Thus, a high internal efficiency was expected. To confirm this, the temperature dependence of the integrated PL intensity was measured under the same conditions as the PL in Fig. 3 and the internal quantum efficiency was evaluated. Figure 4 shows the experimental result and the result for a conventional (0001) $In_xGa_{1-x}N$ QW that emits at a similar wavelength for comparison. The internal quantum efficiency at low temperatures was regarded as 100% and that of the {11$\bar{2}$2} QWs at RT was estimated 33%, which, as expected, is about twice as high as in the (0001) QW. In addition, steep thermal quenching has not been observed on the long wavelength side of the PL spectrum, which suggests the high internal quantum efficiency is nearly independent of the emitting wavelength. Although the maximum internal quantum efficiency achieved in the red spectral range by $In_xGa_{1-x}N$ based LEDs thus far is a few percent, a red component in our {11$\bar{2}$2} QW shows a high internal quantum efficiency. Possible reasons for this are weaker internal electric fields and a well thickness as thin as 2 nm. This thin well thickness prevents misfit dislocations from being introduced into the QW even with a high In composition, that is, in the region emitting red.

Our previous theoretical study[11] showed that the exciton spontaneous-emission lifetime is strongly affected by the presence of electric fields. Therefore, if the internal electric fields in the {11$\bar{2}$2} QW are weakened, then a fast radiative recombination lifetime should be observed. To demonstrate this, time-resolved PL (TRPL) measurements were performed at 13 K with the same excitation conditions as above. Figure 5 shows the PL decay curves at 460 nm (blue), 530 nm (green), and 575 nm (amber) within the broad {11$\bar{2}$2} QW emission. Each curve is composed of fast and slow decays, but their interpretation is rather complicated because carrier/exciton transfer due to the In distribution may occur in the present QW. Therefore, we have yet to draw a conclusion. However, comparing to the decay observed for the reference (0001) QW that emits green, it is clear that all the decay components in the {11$\bar{2}$2} QWs possess much faster lifetimes, which strongly suggests much faster radiative recombination lifetimes due to weakened internal electric fields. Again we like to emphasize that the amber component also possesses quite fast lifetimes, but the PL decay for nitride-based red LEDs is usually on the order of microseconds. Thus, the improved internal quantum efficiency even in the long wavelength range can be attributed to the drastically fast radiative lifetimes.

One characteristic of conventional light-emitting devices, including nitride–semiconductor-based emitters, is that they provide nearly monochromatic output light. This is suitable for display devices based on the red-green-blue trichromatic system, but is unfavorable to (solid state) lighting as monochromatic light degrades the color-rendering properties. In this paper, we demonstrated that the rainbow color luminescence can be realized by the {11$\bar{2}$2} QW fabricated by the regrowth technique and that the internal quantum efficiency is always high within the emission spectra. Furthermore, the apparent color is controlled by the growth conditions. These properties make us believe that our proposed structure is promising for light-emitting devices that require sophisticated syntheses of colors such as pastels and white.

The authors acknowledge the Venture Business Laboratory in Kyoto University (KU–VBL) and the 21st Century COE Program (Grant No. 14213201).

[1]J. Wu, W. Walukiewicz, K. M. Yu, J. W. Ager III, E. E. Haller, Hai Lu, William J. Schaff, Y. Saito, and Y. Nanishi, Appl. Phys. Lett. **80**, 3967 (2002).
[2]T. Matsuoka, H. Okamoto, M. Nakao, H. Harima, and E. Kurimoto, Appl. Phys. Lett. **81**, 1246 (2002).
[3]P. Perlin, C. Kisielowski, V. Iota, B. A. Weinstein, L. Mattos, N. A. Shapiro, J. Kruger, E. R. Weber, and J. Yang, Appl. Phys. Lett. **73**, 2778 (1998).
[4]T. Takeuchi, S. Sota, M. Katsuragawa, M. Komori, H. Takeuchi, H. Amano, and I. Akasaki, Jpn. J. Appl. Phys., Part 2 **36**, L382 (1997).
[5]P. Waltereit, O. Brandt, A. Trampert, H. T. Grahn, J. Menniger, M. Ramsteiner, M. Reiche, and K. H. Ploog, Nature (London) **406**, 865 (2000).
[6]H. M. Ng, Appl. Phys. Lett. **80**, 4369 (2002).
[7]T. Onuma, A. Chakraborty, B. A. Haskell, S. Keller, S. P. DenBaars, J. S. Speck, S. Nakamura, U. K. Mishra, T. Sota, and S. F. Chichibu, Appl. Phys. Lett. **86**, 151918 (2005).
[8]T. Takeuchi, A. Amano, and I. Akasaki, Jpn. J. Appl. Phys., Part 1 **39**, 413 (2000).
[9]S-H. Park, J. Appl. Phys. **91**, 9904 (2002).
[10]K. Nishizuka, M. Funato, Y. Kawakami, Y. Narukawa, T. Mukai, and Sg. Fujita, Appl. Phys. Lett. **85**, 3122 (2004).
[11]M. Funato, Y. Kawaguchi, and Sg. Fujita, Mater. Res. Soc. Symp. Proc. **798**, 347 (2003).